

Traffic smoothing using explicit local controllers

Dissipating Stop-and-Go Waves with a Single Automated Vehicle in Dense Traffic:
Experimental Evidence

AMAURY HAYAT[†], ARWA ALANQARY^{*,1}, RAHUL BHADANI^{§, 1}, CHRISTOPHER DENARO^{‡,1}, RYAN J. WEIGHTMAN^{‡,1}, SHENGQUAN XIANG^{||,1}, JONATHAN W. LEE^{*}, MATTHEW BUNTING[‡], ANISH GOLLAKOTA^{*}, MATTHEW W. NICE[‡], DEREK GLOUDEMANS[‡], GERGELY ZACHÁR[‡], JON F. DAVIS^{*}, MARIA LAURA DELLE MONACHE^{*}, BENJAMIN SEIBOLD^{**}, ALEXANDRE M. BAYEN^{*}, JONATHAN SPRINKLE[‡], DANIEL B. WORK[‡] AND BENEDETTO PICCOLI[‡],

^{*}–University of California, Berkeley

[†]–École des Ponts Paristech, Marne la Vallée

[‡]–Vanderbilt University

^{||}– Peking University

[§] – The University of Alabama in Huntsville

^{**}–Temple University

^{‡‡}–Rutgers University-Camden

¹–These authors contributed equally

Abstract

The dissipation of stop-and-go waves attracted recent attention as a traffic management problem, which can be efficiently addressed by automated driving. As part of the 100 automated vehicles experiment named MegaVanderTest, feedback controls were used to induce strong dissipation via velocity smoothing. More precisely, a single vehicle driving differently in one of the four lanes of I-24 in the Nashville area was able to regularize the velocity profile by reducing oscillations in time and velocity differences among vehicles. Quantitative measures of this effect were possible due to the innovative I-24 MOTION [19] system capable of monitoring the traffic conditions for all vehicles on the roadway. This paper presents the control design, the technological aspects involved in its deployment, and, finally, the results achieved by the experiment.

1 Introduction

Stop-and-go waves are ubiquitous traffic instabilities observed in almost all parts of the world [41, 30]. The drawbacks of such waves include increased fuel consumption and decreased safety [38]. Taming or dissipating them is a problem of traffic management. The latter has witnessed a revolution with the technical capability of replacing fixed control actuators (for example, toll gates, traffic lights, and traffic signals) with mobile actuators such as connected and automated vehicles (AVs). Researchers studied the capability of this control paradigm to regulate traffic, including dissipating waves, even if most results are for the case of high penetration of AVs (high percentage of AVs as part of the bulk traffic) or completely autonomous traffic. Simulation results can be found in [11, 40, 23, 43]. Other strategies included variable speed limit strategies, [4, 44, 24] and jam absorption [35, 28]. The modeling of the problem generates some interesting mathematical challenges, such as the need for multiscale models [14].

In the last few years, some experimental results have become available [38, 50, 37]. In particular, the ring-road experiment described in these papers shows how a single AV can tame waves produced by 21 human-driven

vehicles. The experiment setup replicated faithfully the seminal one described in [39]: 22 vehicles started at equal distances on a circular track of 260 meters and reached the same speed. After a short time, stop-and-go waves naturally appear but the single AV is able to dissipate them. These results were achieved originally by the controller described in [7]. Continued research has explored either model-based techniques [1, 12, 16, 26, 29] or AI ones [33, 42, 49, 48, 47, 51]. The encouraging results included a decrease in speed variance, reduced fuel consumption, and reduced heavy braking. In this experiment, drivers were instructed to close the gap while driving safely but with no knowledge of the experiment’s goals. This reduced the potential biases but limitations remained: the confined setting, the single-lane situation, and the artificial environment.

In order to move forward to an open highway, a holistic vision was proposed [25, 31] based on an innovative monitoring camera system [19], the use of advanced hardware devices [10, 5, 34], energy modeling and control algorithms. The approach consisted of inserting 100 automated vehicles in bulk traffic and using various control algorithms. The controller presented in this paper was used on a single vehicle out of the 100. Since the expected penetration rate was around 1-3%, each AV was surrounded by 30-100 human-driven vehicles. With this in mind, the key problem was that of designing controls for a single AV in a multilane setting (with no lane-changing maneuvers), which would impact traffic while maintaining requirements for safety. As for the ring-road experiments, the focus was on smoothing traffic via reduced speed variance. Also, in this setting, the smoothed traffic was expected to be more fuel-efficient and safe than oscillating ones and stop-and-go waves.

In this paper, we present the experimental evidence that a single automated car equipped with an appropriate model-based controller can efficiently dissipate a stop-and-go wave in open traffic on the highway. This experiment was carried out in November 2022 as part of the MegaVanderTest that took place on I-24 in Nashville, TN, described further in [2]. The highway includes freight traffic, exhibits stop-and-go traffic daily during rush hour, and includes more than 150,000 vehicles daily. This is the ideal situation for testing the controls and the general idea of traffic smoothing via a small number of AVs.

We first present the controller we used, which was designed from mathematical principles using a microscopic traffic model [26]. To smooth traffic while ensuring safety, the controller was designed as a combination of three parts: a safety module, a target speed, and a Model Predictive Control (briefly MPC) component. The safety module computes the maximal speed, which would allow the AV to avoid collision in case of sudden braking of the leading vehicle (directly in front of the AV). The target speed is the expected uniform speed the smoothed traffic will travel at. Such speed is either decided using global information (speed planner) or local traffic velocity. Finally, the Model Predictive Control component is designed to anticipate the speed changes of the leader vehicle while keeping the speed as close as possible to the target ones.

This paper goes beyond the theoretical development of the controller. It demonstrates implementation on a full-sized car, deployed in traffic as a moving traffic wave controller. The experiment was conducted as part of the MegaVanderTest. The deployment was on the westbound I-24 highway to Nashville, TN, on Wednesday, November 16th, during morning rush hour (8-9 am), on a 9.33-kilometer stretch between exits 66 and 60. We analyze the results using the trajectories reconstructed by the I-24 MOTION system [19]. Each car trajectory was obtained through processing and analysis of video data from the myriad cameras of I-24 MOTION (see I-24 MOTION).

Since our aim was traffic smoothing via speed oscillation reduction, we focused on computing the speed variance along trajectories. More specifically, the effect of the AV control is measured by comparing the speed variance of the cars running in front of the AV (thus not subject to the control) with those of the cars running behind the AV. A direct effect can be visually noted by comparing the lane where the AV traveled with other lanes (see Figure 4).

We demonstrate our results by calculating and comparing speed variance. The speed variance over 1.4 km behind the AV was 50% less than the speed variance in front. A more detailed analysis, see Table 1, reveals that such impact is stronger in the vicinity of the AV (200 to 400 m). Indeed oscillations are observed to appear again around 600 m behind the AV. This length has to be compared with the ring-road experiment of [38, 50, 37], where oscillations were completely removed on a length of 260 m. In simple words, the AV obtained a similar effect on an open highway with a strong effect for around double the size of the ring road. In the remainder of this paper, we will carefully review the design, implementation, deployment, and analysis of our experiment and its results. The paper will show how a carefully crafted model-based acceleration

controller was able to smooth traffic on an open highway with dense traffic and four lanes. The main result is the cut in half the speed oscillations between vehicles in front and behind the AV. Moreover, the controller used standard sensor measurements from stock ACC systems on commercially available Toyota Rav4 models, thus opening the door to large-scale implementation.

Control theory, stabilization... and road traffic

by Amaury Hayat and Shengquan Xiang

Control theory in a nutshell...

Control theory is about asking: “If I can act on the system, what can I make it do?”. From a mathematical point of view, it consists of having a system

$$\dot{x}(t) = f(x(t), u(t)), \quad (1)$$

where $x(t)$ is the state and $u(t)$ is a function –called control– that can be chosen and represent the way we can act on the system. A typical goal in control theory is to know, given an initial state x_0 , what states x_1 can be reached by choosing $u(t)$ properly.

Stabilization is a sub-branch of control theory where the goal is to make sure that the system follows a target state \bar{x} and returns to it when disturbed. A control is designed to stabilize a system that would be unstable in the absence of a controlling force. That is to say

$$\left\{ \begin{array}{l} \text{for any } \varepsilon > 0, \text{ there exists } \eta \text{ s.t. for all } t \in [0, +\infty) \\ \|x(0) - \bar{x}(0)\| \leq \eta \implies \|x(t) - \bar{x}(t)\| \leq \varepsilon, \end{array} \right. \quad (2)$$

$$\exists \delta > 0 \text{ s.t. } \|x(0) - \bar{x}(0)\| \leq \delta \implies \lim_{t \rightarrow +\infty} \|x(t) - \bar{x}(t)\| = 0. \quad (3)$$

Most of the time, \bar{x} is chosen as a constant and is an equilibrium of the system, that is

$$f(\bar{x}, 0) = 0. \quad (4)$$

The particularity of stabilization is that the control $u(t)$ does not depend on the initial condition x_0 but rather on the current state $x(t)$, that is formally

$$u(t) = g(x(t)). \quad (5)$$

In more general versions $u(t)$ could also depend on past state $(x(\tau))_{\tau \leq t}$. A control in this form is called a *feedback law*.

...and in road traffic

In road traffic, using an AV to smooth stop-and-go waves enters the following framework: $x(t)$ represents the state of the cars on the road, for instance, their position h_i and velocity v_i . The control $u(t)$ is the acceleration or the velocity of the AV that can be chosen, up to some safety and hardware constraints. Formally, this can be written as

$$\underbrace{\dot{x}(t)}_{\text{traffic state}} = f(x(t), \underbrace{u(t)}_{\text{AV dynamic}}). \quad (6)$$

$\underbrace{\hspace{10em}}_{\text{traffic dynamic}}$

The target state \bar{x} is the uniform flow equilibrium where every car is going the same constant speed. This target state is unstable in congestion when there is no controlled AV, meaning that $x(t)$ is usually far from its equilibrium value \bar{x} . An example of such a system in traffic is, for instance (see [3, 15, 26, 22])

$$\begin{cases} \dot{v}_0 = u(t), \\ \dot{y}_0 = v_0, \\ \dot{v}_i = a \frac{v_{i+1} - v_i}{(y_{i+1} - y_i)^2} + b[V(y_{i+1} - y_i) - v_i], \\ \dot{y}_i = v_i, \end{cases} \quad (7)$$

Smoothing stop-and-go waves simply amounts to choosing u to reduce

$$\int_0^T \|x(t) - \bar{x}\| dt,$$

where the state is $x(t) = (y(t), v(t))$ and T is a given time horizon. In practice, there are several difficulties:

- (i) The target state \bar{x} (and in particular the target speed) is usually unknown in practical cases such as a highway. Two ways to tackle this difficulty can be thought of:
 - Infer a good approximation of \bar{x} from both theory and experimental measurements. This is, in part, the principle of the speed planner presented below (see Hierarchical Control Framework and Speed Planner);
 - Aim to reduce the variance of x with respect to time instead of aiming to reduce $\|x(t) - \bar{x}\|$.
- (ii) The dynamic f is quite complicated because of the lane changes: the system is usually either *infinite dimensional* or *hybrid*.
- (iii) The mathematical models representing road traffic are usually imprecise. Thus the control needs to be robust with respect to errors on f .
- (iv) The control system must exhibit robustness in handling errors related to measurements, including signal loss, sensor and camera limitations, etc.

2 Controller design

From a control theory perspective, the approach consists of considering a connected AV as a means of control on the system, that is, the whole traffic flow. The controller is acceleration-based, meaning that the control variable is the acceleration of the connected AV. In this section, we describe the AV's acceleration-based controller based on the design described in [27].

2.1 Principle

The controller combines three components:

- **Safety**, a module that ensures that the vehicle never puts itself or others in danger.
- **Target**, a module that calculates the target speed required to achieve the control goal.
- **Model Predictive Control (briefly MPC)**, a module that anticipates the leader's behavior to help limit the AV's speed deviations from the target speed.

Each of the modules leads to a limit acceleration respectively denoted by a_{safe} , a_{target} , a_{MPC} . The controller combines these three limit accelerations by taking their minimum. The commanded acceleration of the controller can be written at each time as:

$$a_{\text{cmd}}(t) = \min(a_{\text{safe}}(t), a_{\text{target}}(t), a_{\text{MPC}}(t)), \quad (8)$$

The mathematical expression of $a_{\text{safe}}(t)$, $a_{\text{target}}(t)$ and $a_{\text{MPC}}(t)$ are detailed in the following paragraphs.

2.2 Notations

We introduce the following notations for these time-varying signals:

- v refers to the instantaneous driving speed of the AV (or ego vehicle).
- v_{lead} is the measured speed of the leader vehicle.
- h is the space gap between the ego vehicle and the leading vehicle.
- v_{rel} is the relative speed of the leader with respect to the ego vehicle.
- a is the measured estimate of acceleration of the ego vehicle.
- a_{lead} is the actual acceleration of the leading vehicle.

2.3 Safety Module

We first define v_{safe} as the highest velocity below which the AV can remain safe by braking if needed, whatever the behavior of the leading vehicle. Under this velocity, even if the leader brakes extremely strongly until full stop, the AV can avoid collision.

This $v_{\text{safe}}(t)$ is a computed value at any time t , depending on the space gap $h(t)$, the maximal braking capacity of the AV (a constant, denoted $a_{\text{min}} < 0$), and the maximal braking capacity of the leading vehicle (a constant denoted $a_{l,\text{min}} < 0$). This velocity can be computed explicitly and is given by (see [27, Theorem 1.1])

$$v_{\text{safe}}(t) = \sqrt{2|a_{\text{min}}| \left(h(t) - s_0 + \frac{1}{2} \frac{v_{\text{lead}}^2(t)}{|a_{l,\text{min}}|} \right)}, \quad (9)$$

where $s_0 > 0$ is a given safety distance. The acceleration $a_{\text{safe}}(t)$ is then defined as

$$a_{\text{safe}}(t) = -k(v(t) - v_{\text{safe}}(t)) + \frac{dv_{\text{safe}}(t)}{dt}, \quad (10)$$

where $k \in \mathbb{R}^+$ is a given positive parameter. This acceleration acts as a barrier and guarantees the safety of the AV (provided that it starts in the safe area and no unsafe lane changes happen, see [27, Theorem 1.1]).

2.4 Target Module

The acceleration $a_{\text{target}}(t)$ is defined as

$$a_{\text{target}}(t) = -k(v(t) - v_{\text{target}}(t)), \quad (11)$$

where $v_{\text{target}}(t)$ is a target velocity chosen at time t to reach the control goal. The choice of this target velocity depends on the availability of the downstream information. We consider two modes:

Local mode When there is no downstream information available, either because there is no source or because of a defect in the connectivity of the AV, the target speed is chosen from the only information available, that is, the velocity of the leading vehicle, the one of the AV, and the space gap. In this case, the

goal is to use this information to reconstruct an approximation of what would be the steady-state speed if there were as many vehicles but no stop-and-go wave. This speed is chosen as follows

$$v_{target}(t) = \bar{v}_{lead}(t) + c_1 \frac{\max(0, c_2(h(t) - \delta_1 v(t)))}{\max(1, v(t))^2}, \quad (12)$$

where

$$\bar{v}_{lead}(t) = \begin{cases} \frac{1}{t} \int_0^t v_{lead}(s) ds, & \text{if } t \leq \tau, \\ \frac{1}{\tau} \int_{t-\tau}^t v_{lead}(s) ds, & \text{if } t > \tau, \end{cases} \quad (13)$$

and c_1 , δ_1 and τ are design parameters that can be chosen and have the following interpretation:

- c_1 is a catching-up weight,
- δ_1 is a target time gap between the ego and the leading car,
- τ is an approximation of the period of a stop-and-go wave.

Planning mode When downstream information is available, we use the speed planner described in Hierarchical Control Framework and Speed Planner to get an estimation of the target speed for the current location of the ego vehicle based on the downstream traffic information. We denote this speed by $v_{down}(t)$, and we use it as our target speed after clipping it to be within some factor of the leader speed and ensure that it does not exceed a reference upper-bound speed v_{ref} . That is

$$\bar{v}_{target}(t) = \max(\max(v_{down}, \alpha_0 v_{lead}(t)), \min(\alpha_1 v_{lead}(t), v_{ref})), \quad (14)$$

where $\alpha_0 \in (0, 1)$ and $\alpha_1 > 1$ are design parameters and v_{ref} is a reference velocity which corresponds to a safeguard when we know an upper bound of the traffic speed in congestion. If no such bound is known, v_{ref} is simply set to the road speed limit.

2.5 MPC Control

The MPC control is the most complex part. It is designed to anticipate the leader's behavior and restrict the AV's deviation from its target speed. The paradigm is: to react quickly to a change in the leader's behavior, but as little and smoothly as possible.

To do so, when the leading vehicle decelerates, the acceleration a_{MPC} commanded by the MPC module is set as the smallest possible deceleration such that the AV will remain safe in terms of collision: in other words, it would not reach the safety distance, should the leader keep its constant deceleration until full stop. To compute this value, we define the acceleration $a_{min\ brake}$ as:

$$\begin{aligned} & a_{min\ brake}(h(t), v(t), v_{lead}(t), a_{lead}(t)) \\ &= - \left(h(t) - s_0 + \frac{1}{2} \frac{v_{lead}^2(t)}{-a_{lead}(t)} \right)^{-1} \frac{(v(t))^2}{2}, \end{aligned} \quad (15)$$

and the quantities

$$P_1 = a_{min\ brake}(h(t), v(t), v_{lead}(t), a_{lead}(t)) - a_{lead}(t)v(t)/v_{lead}(t), \quad (16)$$

$$P_2 = v_{lead}(t) - v(t). \quad (17)$$

The acceleration a_{MPC} commanded by the anticipation module is

$$a_{MPC} = \begin{cases} a_{min\ brake}(h(t), v(t), v_{lead}(t), a_{lead}(t)), & \text{if } P_1 > 0, \\ a_{lead}v(t)/v_{lead}(t), & \text{if } P_1 \leq 0 \text{ and } P_2 \geq 0, \\ a_{lead} - \frac{(v - v_{lead})^2}{2(h(t) - s_0)}, & \text{if } P_1 \leq 0 \text{ and } P_2 < 0. \end{cases} \quad (18)$$

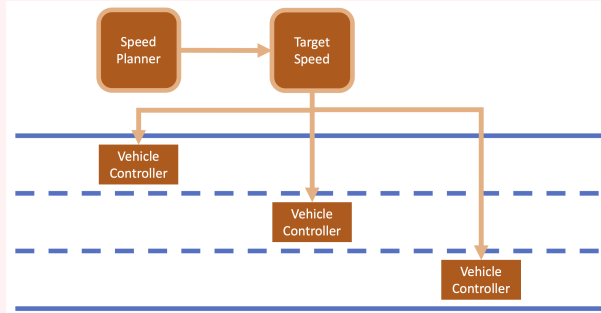
When the leading vehicle speeds up, to avoid any unwanted behavior and jittering we ensure the continuity of the controller by setting

$$a_{MPC} = \begin{cases} a_{\text{lead}} - \frac{(v - v_{\text{lead}})^2}{2(h(t) - s_0)}, & \text{if } P_2 < 0, \\ \min(a_{\text{max}}, a_{\text{lead}}(1 + k_2(v_{\text{lead}} - v))), & \text{if } P_2 \geq 0. \end{cases} \quad (19)$$

More details and a detailed theoretical analysis of this controller can be found in [27].

Hierarchical Control Framework and Speed Planner

by Han Wang



Centralized Speed Planner: the algorithm deployed on the server side that designs target speed profiles for vehicles in moving traffic, with the goal to smooth traffic waves. The system was validated on a fleet of 100 connected automated vehicles in the MVT

The proposed controller served as the vehicle side controller in a novel hierarchical control framework. The framework includes two critical components: 1) the collection of algorithms on the server side operates as the centralized planner agent dealing with the heavy calculation tasks; 2) the algorithms deployed on the vehicle side act as executors following the target assigned by the centralized planner. The principle of the framework design is to solve the computational task allocation problem between the server and the onboard units (OBU) and to efficiently coordinate the control goals between macroscopic traffic flow optimization and microscopic vehicle control.

At the beginning of each update, the speed planner extracts a combination of macroscopic traffic state estimation (TSE) and vehicle observations from the database to calculate the target speed profile. According to the demand and condition of the specific implementation, the speed profile could be published in various formats. Each vehicle's OBU will fetch the most recent target speed from the target speed profile and use it as the input, together with the local observation from the onboard detector's perceptions.

For the Buffer Design module, we consider the interval $\mathcal{I} \subset \mathbb{R}$ as the region of interest. Suppose further that $\mathcal{I}_c \subset \mathcal{I}$ denotes a congested area. The idea is to determine the moving bottleneck (the controlled vehicle) speed profile denoted by $t \mapsto U_b(t)$, such that the density $k(t, x)$ for $x \in \mathcal{I}_c$ is distributed (evenly) throughout the entire region \mathcal{I} and consequently by average the density approaches k_c , the critical density associated with maximum flow. Determining the moving bottleneck speed profile will be done in the following steps: (i) predicting the density $(t, x) \mapsto k(t, x)$, $(t, x) \in \mathbb{R}_+ \times \mathcal{I}$ given a speed profile $U_b(\cdot)$ of the controlled vehicle, using a mathematical model of traffic flow (see the next subsection), (ii) assessing the efficiency of the speed profile $U_b(\cdot)$ based on the density $k(t, x)$ employing the reinforcement learning (RL), and (iii) Updating $U_b(\cdot)$ and returning to step (i).

The vehicle controllers extract information from the target speed and local observation for the control action selection. The local observation will be submitted to the central database as the future input for the speed planner.

2.6 Adaptation to loss of signal

Between the ideal mathematical framework and reality, there are many disturbances and unplanned constraints. To be able to work in real life, the control deployed has to be robust to a number of external perturbations. As underlined in [27], this controller is robust to delay in the measurements or the actuation or to small measurement imprecisions. However, as it stands, this controller is not robust to the loss of signal from the front sensor, which could lead to highly overestimating the space gap and the control to overshoot by far. This loss of signal could be the consequence of a road grade, a curve, or simply a radar malfunction or range limitations. An instance of this was encountered several times during the experiment.

Over and above this problem, the question arises as to what control strategy to adopt when the position of the leading car is unknown for a long period. A simple option would consist of assuming that the leading car has a space gap and velocity that are identical to the last space gap and velocity measured until the signal is reached again. That is to say

$$v_{\text{lead}}(t) = v_{\text{lead}}(t_1), \quad h(t) = h(t_1), \quad \text{for any } t \in [t_1, t_2), \quad (20)$$

where t_1 is the time of the last signal measured and t_2 is the time of the next signal measured. This limits jumps in the behavior of the controlled AV.

However, in *local mode* (see Section *Principle*), this velocity $v_{\text{lead}}(t)$ is used to estimate the ideal steady-state speed of the system. Assuming a constant velocity equal to the last measured velocity of the leading car could bias this estimation by having a strong weight in (13). This could lead to underestimating the real flow speed of the traffic and entering a self-perpetuating situation where the automated vehicle is slower than the traffic and consequently keeps too large a gap to the car in front for the radar to notice. To tackle this issue, for each time step where the signal is lost, we gradually increase the last seen space gap by setting

$$h(t + \Delta t) = h(t) + \Delta t(h_{\text{correction}}). \quad (21)$$

This results in increasing the estimated v_{safe} and \bar{v}_{target} , which in turn allows the ego vehicle to gradually increase its velocity and close the gap to its leader.

In the *planning mode*, we clip the target velocity to be no more than $\alpha_1 v_{\text{lead}}$. So if the leader speed is severely underestimated (due to the lost signal), it can lead to an underestimation of the target velocity. To overcome this, we remove this upper bound on the target speed when the signal is lost and allow it to be larger than the last leader’s speed observed until the signal is regained.

“The controller that combines safety, objectives, and anticipation is capable of operating both with and without downstream information and remains robust even in the event of a signal loss.”

3 Software and hardware implementation

We use a model-based design approach to implement the controller discussed earlier. We can abstract the controller as

$$a_{\text{cmd}}(t) = f(v(t), v_{\text{lead}}(t), h(t), v_{\text{rel}}(t), a(t); \Theta). \quad (22)$$

Recall that v is the instantaneous driving speed of the vehicle to be controlled (ego vehicle), v_{lead} is the measured speed of the leader vehicle, $h(t)$ is the space gap between ego vehicle and its leader, v_{rel} is the relative speed of the leader with respect to the ego vehicle, and a is the acceleration of the ego vehicle. In (22), the controller parameters are represented as Θ . The functional layout of the controller model is given in Figure 1.

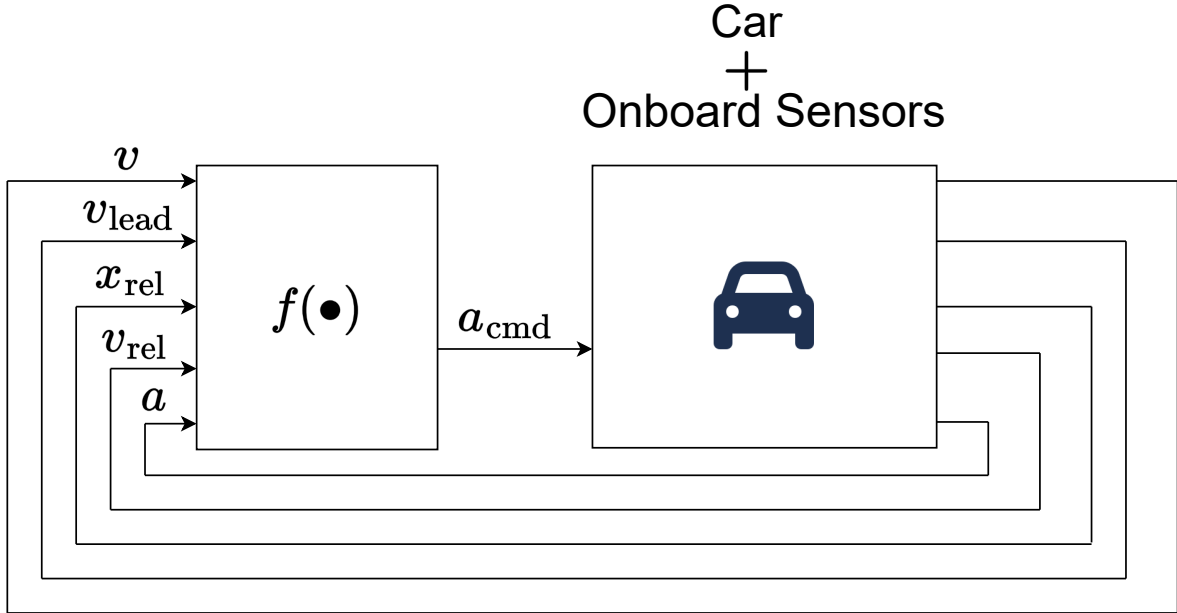


Figure 1: Dataflow layout of the controller in (22), applied to traffic control. The controller is designed for the longitudinal movement of the ego vehicle to follow its leader, which may be a human-driven vehicle.

3.1 Simulink with Code Generation to ROS

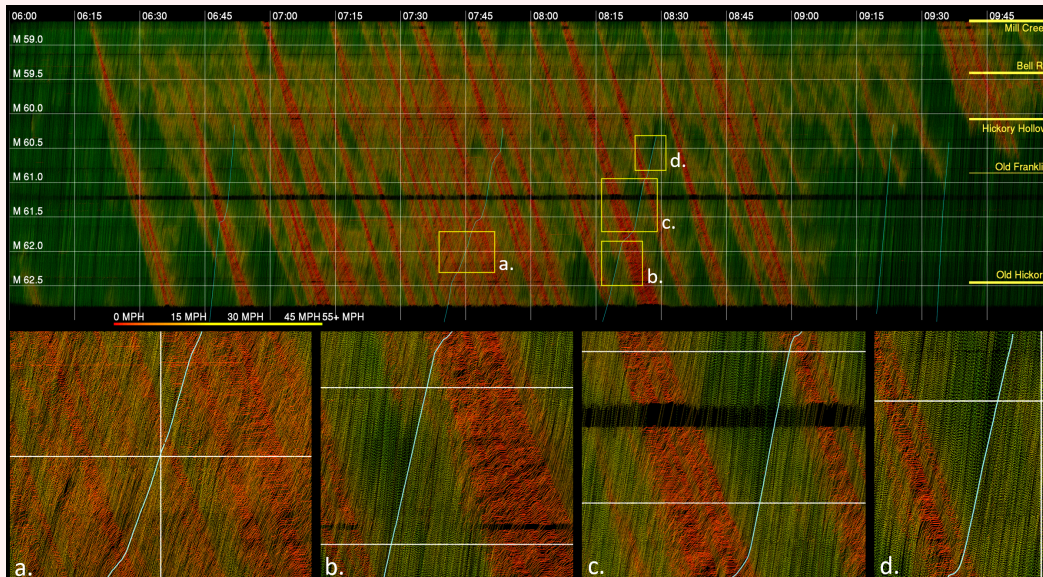
The abstracted controller (22) is implemented as a Simulink model with data input and output components modeled using ROS (Robot Operating System) [36] Toolbox. The Simulink model is used to generate a standalone C++ ROS node that can be executed directly on a physical hardware board without any modification. Moving from the Simulink model to a C++ ROS node without writing any C++ code allows for faster prototyping and validation at an early stage in the simulation through data-driven software-in-the-loop validation of the controller behavior. The ROS node consists of multiple ROS subscribers that consume input data and provide acceleration command output through a ROS publisher [6]. ROS nodes are executed in a parameterized manner through `roslaunch`, a configuration-based tool for ROS that allows the execution of multiple ROS with node parameters supplied at runtime. Validation testing used regression data played back through our Gazebo-based simulator [8], where multi-vehicle simulation uses rigid body dynamics. This allowed us to compare the software deployment candidate with desired performance criteria prior to deploying in hardware.

I-24 MOTION

by Derek Gloudemans, Gergely Zachár, Yanbing Wang, Junyi Ji, Will Barbour, Dan Work

I-24 MOTION [19, 17] is a 4.2-mile instrumented section of I-24 in Nashville, TN. It serves as a traffic data collection instrument and a test bed for connected and automated vehicle technologies and traffic control strategies. The instrumentation consists of 276 4K resolution video cameras mounted on 110-135ft roadside poles. The cameras provide a complete view of the roadway and can observe the path of all vehicles with minimal occlusion.

A video processing pipeline consisting of computer vision [21, 18, 20] and post-processing algorithms identifies and tracks vehicle locations, then stitches [46] and reconciles their trajectories to ensure physical feasibility. The trajectory reconciliation consists of optimization-based smoothing that ensures feasible vehicle dynamics in higher orders [45]. Trajectories are generated in a roadway-aligned curvilinear coordinate system [21] that can be converted to or from GNSS coordinate systems for the purposes of aligning data sources measured from vehicles. From the I-24 MOTION data, multiple traveling traffic waves are regularly observed during morning peak commute times, leading to high-speed variability and consequently increased fuel consumption.



Time-space diagram of traffic trajectories reconstructed from I24-MOTION [19] and visualized with [52], with the AV trajectory overlaid in light blue. Insets show close-ups of traffic near the AV.

3.2 Deployment to Vehicle Platform

The ego vehicle (the test vehicle on which the controller was deployed) was a Toyota RAV4, capable of acceleration-based control using our customized hardware and software stack. As described further in [32] the hardware stack includes Controller Area Network (CAN) transceivers for access to vehicle data (including on-board sensors and actuators) and to inject vehicle commands. The software stack relies on Libpanda [10] to read from hardware. The package strym [5] was used at runtime to decode the on-board data from the CAN, and the CAN_to_ROS package [13, 34] was used to transmit data into ROS for producers/consumers of vehicle data. This included the ability to share the live view of the vehicle’s state and to allow automatic upgrades, as described in [34]. All of the software and hardware are integrated through a Raspberry Pi, enabling a cost-effective means to retrofit the vehicle for data acquisition and control.

The role of Libpanda and CAN_to_ROS is illustrated in Figure 2. The vehicle interface node in CAN_to_ROS subscribes to the commanded acceleration topic, and converts the required command to CAN messages that are sent over to the vehicle via CAN peripherals for actuation. A more detailed description of the controller implementation can be found in [6].

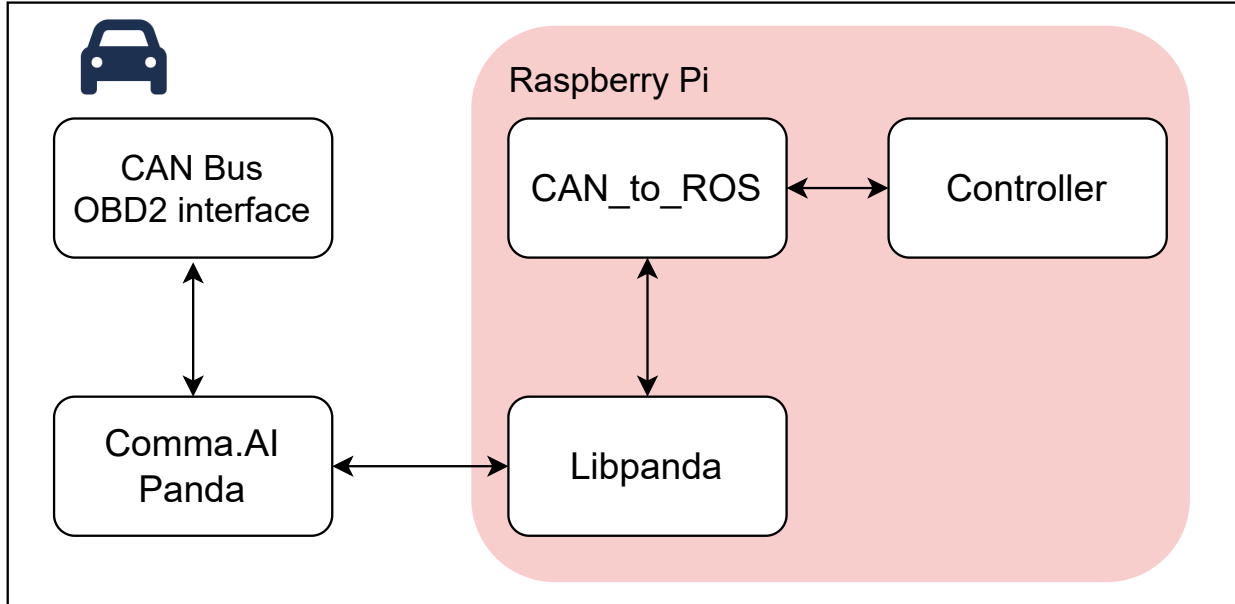


Figure 2: A functional layout of the controller for car-following strategy in a mixed-autonomy traffic experiment. The controller is designed for the longitudinal movement of the ego vehicle to follow its leader, which may be a human-driven vehicle.

4 Framework of the experiment

The controller was deployed on a Toyota RAV4 in dense traffic on a segment of the four-lane westbound I-24 highway to Nashville, TN (see Figure 3). The experiment was carried out on Wednesday, November 16th, during the morning rush hour. The results presented in this paper are collected between 08:10 am and 08:50 am. During this time, the AV was traveling westbound between exits 66 and 60 for a total distance of 9.33 km and was located in lane 3, where lane 4 denotes the rightmost lane and lane 1 denotes the leftmost lane. During the experiment runs, the controller sets the desired acceleration of the vehicle, but only when Adaptive Cruise Control (ACC) is enabled and engaged: thus, the driver interface is the same as they would normally expect. Vehicle design features allow the controller to initially engage once the vehicle is driving above 20mph . The driver engaged the controller as soon as the vehicle is driving above this limit on the highway. Both in stock ACC and with this controller, some events can trigger the controller to disengage without the driver’s input. For instance, a close cut-in in front of the ego vehicle or following a very strong deceleration by the lead vehicle. In this case, the driver establishes as soon as possible, while under human control, an appropriate gap that allows for re-engaging the controller. In instances where the average speed of traffic was expected to be less than 20mph for some time due to congestion and the controller disengaged for one of the reasons above, the driver was asked to manually follow the commanded values asked by the controller with the help of the on-board computer monitored by a researcher on the passenger seat until it could be re-engaged.

Data from the experimental runs are collected in two ways. The CAN data from the ego vehicle is logged in a database as in [9]. More importantly, the trajectories of the AV and surrounding vehicles are recovered from video footage recorded and processed by I-24 MOTION [19] to extract the trajectories. A brief description

of the I-24 MOTION system and data set can be found in I24-MOTION and more details can be found in [19], in particular concerning the reconstruction procedure of the trajectories. The AV trajectory obtained from the camera is then synchronized with the AV trajectory from the CAN data to avoid any spatial offset due to GPS imprecision.



Figure 3: The experiment took place on the westbound of the I-24 between exits 66 and 60 with a total distance of approximately 9.33 km.

“We present experimental evidence that an AV running a model-based controller can locally dissipate a stop-and-go wave in heavy traffic on the highway.”

5 Results

In this section, we present the experimental results of the controller on the test run described in 4 section. These results show evidence that the single AV deployed in dense traffic improves the performance of the system locally. We will exhibit its effect qualitatively by looking into the time-space diagrams in the vicinity of the AV. We will also quantify the effect using the speed variance.

5.1 Time-space diagrams.

In Figure 4 (a), we show the trajectories of the AV and the surrounding vehicles in the same lane (lane 3) through a single wave. We include trajectories up to 800 *m* upstream of the wave bottleneck. The trajectories in black denote the vehicles behind the AV, while the trajectories in blue are the vehicles in front of the AV.

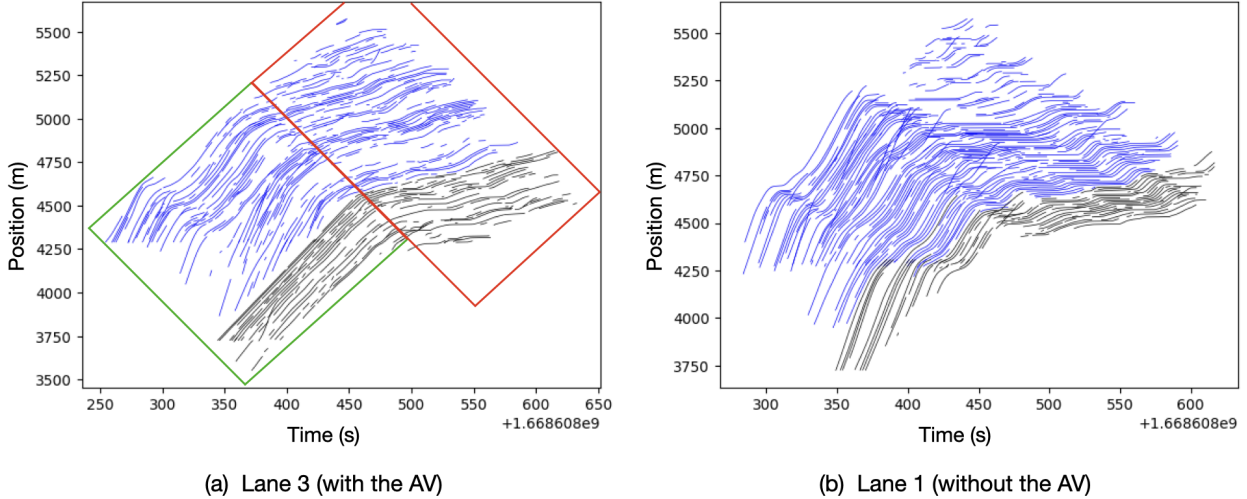


Figure 4: Time-space diagrams showing the trajectories of the vehicles up to 400 m upstream (black) and up to 1400 m downstream (blue) of the AV on two different lanes. **(a)**: The trajectories are shown from the AV’s lane (lane 3). **(b)**: The trajectories are shown from another lane without an AV (lane 1). The green box on figure (a) indicates the region where the AV completely absorbs the wave

We show trajectories up to 1400 m in front of the AV and 400 m behind it. Because the wave propagates backward in time, we need to identify the moving border of the wave. The procedure to do so is detailed in Appendix A.

In Figure 4 (b), we show the trajectories of the vehicles in the same time-space region of the identified wave in a different lane (lane 1), which does not contain any AVs. We use lane 1 for comparison (instead of the adjacent lane 2) to reduce the possible spillover effect of the AV on adjacent lanes. Similarly, in this figure, the black trajectories denote the vehicles upstream of the x -position of the AV, while blue trajectories are the downstream vehicles.

From Figure 4 (a), we notice that the blue trajectories in front of the AV experience speed oscillations due to the propagation of waves similar to Figure 4 (b). However, the effect of the AV is apparent on the vehicles behind it (black trajectories). In the region upstream the bottleneck (the green box of Figure 4 (a)) the oscillations are completely absorbed by the AV and do not propagate to the vehicles behind it. In this region, we notice that the AV is driving with a steady speed despite the stop-and-go behavior in front of it. The trailing vehicles’ behavior is closely aligned with the AV’s as they also exhibit much less speed variations. The AV eventually catches up with the bottleneck (the red region of the time-space diagram) and has to slow down, indicating that it is traveling faster than the bottleneck.

In contrast, we notice from Figure 4 (b) that in the absence of the AV, the wave propagates throughout the entire region. We observe several stop-and-go oscillations that affect all the vehicles in that region.

5.2 Speed Variance

To explore the smoothing effect of the AV, we compare the speed variance of the vehicles behind the AV to those in front of the AV. We use the trajectories shown in Figure 4 (a) to compute the speed variance where the variance is computed across all cars and all time steps (for the vehicles in front and behind the AV separately). The speed variance of the trajectories **in front** of the AV is $19.6 \text{ m}^2 \cdot \text{s}^{-2}$ while the speed variance for the trajectories **behind** the AV is $9.4 \text{ m}^2 \cdot \text{s}^{-2}$. The introduction of the AV has a smoothing effect that reduces the speed variance by **52%**. This is aligned with the observed behavior in the time-space diagram is 4 (a).

Distance behind AV \ Distance in front of AV	1400m	1200m	1000 m	800m	600m	400m	200m
200m	-58%	-58%	-59%	-62%	-67%	-71%	-74%
400m	-52%	-52%	-53%	-56%	-62%	-66%	-70%
600m	-52%	-51%	-52%	-56%	-62%	-66%	-69%
800m	-41%	-40%	-41%	-46%	-53%	-59%	-63%
1000m	-22%	-22%	-23%	-30%	-39%	-46%	-51%
1200m	-11%	-10%	-12%	-19%	-30%	-38%	-44%
1400m	+5%	+6%	+5%	+4%	-17%	-27%	-34%

Table 1: Percentage change of speed variance of the vehicles behind the controlled AV compared to the vehicles in front of it up to different distances.

5.3 Discussion

The results presented in the previous section clearly demonstrate that the proposed controller has a substantial impact on dissipating stop-and-go waves and reducing speed variance. Even in the most bottleneck part of the wave (the red region in Figure 4 (a)), where one might assume that the controller’s impact is minimal, the speed variance in front of the AV is $1.73 m^2 \cdot s^{-2}$ while it reduces to $1.08 m^2 \cdot s^{-2}$ due to the AV’s smoothing effect.

Our analysis thus far focuses on the vehicles within 400 m behind the AV. It is worth noting that the effect of the AV diminishes with the distance. In Figure 5, we extend the 400 m to 1400 m to observe the behavior of the vehicles driving further behind the AV. We notice that speed oscillations start to reappear after around 600 m behind the AV. We made this observation more concrete by reporting the speed variance of the vehicles behind the AV up to different distances ranging from 200 m to 1400 m in Figure 6. We notice a sharp increase in the speed variance after 600m. Furthermore, we report the percentage change in the speed variance considering different distances behind and in front of the AV in Table 1.

Finally, in Figures 8 and 9 we illustrate the physical vehicle and the research team that executed the experiment.

6 Conclusion

We presented an acceleration-based controller for a connected AV to smooth stop-and-go waves in highway traffic. The controller was implemented on a commercially available Toyota Rav 4, using measurements typically used by the Automated Cruise Control. The vehicle was deployed on the I-24 in the Nashville area in bulk traffic during rush hours, as part of a large-scale experiment. Trajectories were reconstructed thanks to the I-24 MOTION system using 276 high-fidelity cameras. The experimental results show the control ability to dampen stop-and-go waves in real traffic at peak hours. The controlled AV reduces the overall speed variance of the traffic up to 600 m behind by around 50%.

7 Acknowledgement

This material is based upon work supported by the National Science Foundation under Grants CNS-1837244 (A. Bayen), CNS-1837652 (D. Work), CNS-1837481 (B. Piccoli), CNS-1837210 (G. Pappas), CNS-1446715 (B. Piccoli), CNS-2135579 (D. Work, A. Bayen, J. Sprinkle, J. Lee) as well as the IEA project SHYSTR and the PEPS JCJC 2022 of CNRS INSMI (A. Hayat and S. Xiang). This material is based upon work supported by the U.S. Department of Energy’s Office of Energy Efficiency and Renewable Energy (EERE) under the Vehicle Technologies Office award number CID DE-EE0008872. The views expressed herein do not necessarily represent the views of the U.S. Department of Energy or the United States Government.

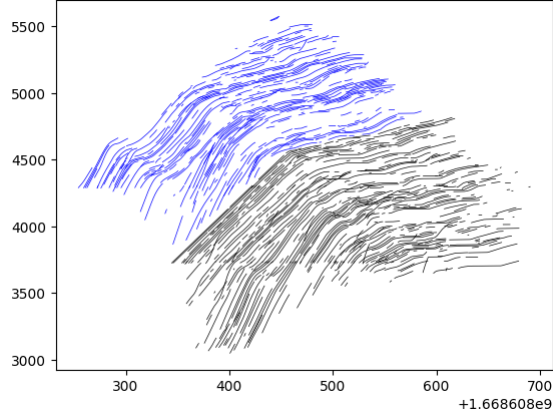


Figure 5: Time-space diagrams showing the trajectories of the vehicles up to 1500 m upstream (black) and up to 1400 m downstream (blue) of the AV.

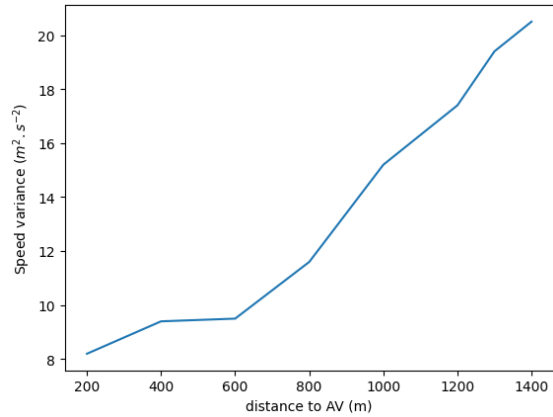


Figure 6: Speed variance of the vehicles behind the AV up to different distances.

A Identifying moving border of the wave

To identify the moving border of the wave for the cars in front and behind the AV we proceed as follows:

1. Define how far in front of the AV and how far behind the AV to consider (for example, 1500m in front, 700m behind)
2. Discretize the space in front and behind the AV in **boxes** of same width following the contour of the AV trajectory and ordered by distance to the AV (for example box 1 contains all trajectories starting between 0m and 200m from the AV, box 2 all trajectories starting between 200m and 400m, etc.).
3. Define a time-axis length to discretize each **box** with time (for example 10s)
4. For each **box**, create *sub-boxes* by using the time-axis discretization length. With a 10s time discretization and a 200m space discretization, this results in 10s by 200m *sub-boxes* for each *box* following the contour of the AV trajectory)
5. For a given **box**, compute the average speed and position of the vehicles in each *sub-box*. Optionally, use a moving average to smooth these values within the **box**.
6. Define a *speed threshold* which will determine when the congested part of the wave begins or ends (for example 4 meters per second)

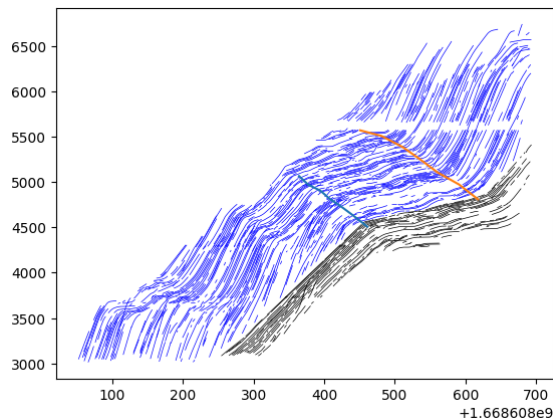


Figure 7: **Automatic identification of the congested part of the wave.** The frontiers of the congested part of the wave are represented in blue and orange. We display all the trajectories located within 1500m in front of the AV and 400m behind.



Figure 8: Test run on Wednesday November, 16th. The driver is assisted by a researcher visualizing and monitoring the control in real-time.

7. For each *box*, iterate over the *sub-boxes*, and compare the average speed in the current *sub-box* to the average speed of the previous *sub-box* and the *speed threshold*. If the current average speed is less than the *speed threshold* and the previous average speed is greater than the *speed threshold*, denote the current *sub-box* as the beginning of the wave. If the current average speed is greater than the *speed threshold* and the previous average speed is less than the *speed threshold*, denote the current *sub-box* as the end of the wave.
8. For each *box*, define the boundary of the wave using the average time and average position of the *sub-boxes* denoting the start and end of the wave. Optionally smooth the obtained frontiers using a moving average.

With 200m and 10s space and time resolution, this results in the identification of the congested part of the wave represented in Figure 7



Figure 9: Follow-up run on Thursday November 17th. The driver activated the controller whose activity is monitored on a computer by the passenger

References

- [1] Saleh Albeaik, Alexandre Bayen, Maria Teresa Chiri, Xiaoqian Gong, Amaury Hayat, Nicolas Kardous, Alexander Keimer, Sean T McQuade, Benedetto Piccoli, and Yiling You. Limitations and improvements of the intelligent driver model (idm). *SIAM Journal on Applied Dynamical Systems*, 21(3):1862–1892, 2022.
- [2] Mostafa Ameli, Sean McQuade, Jonathan W. Lee, Matthew Bunting, Matthew Nice, Han Wang, William Barbour, Ryan Weightman, Denaro Chris, Ryan DeLorenzo, Sharon Hornstein, Jon F. Davis, Dan Timsit, Riley Wagner, Rita Xu, Malaika Mahmood, Mikail Mahmood, Maria Laura Delle Monache, Benjamin Seibold, Daniel B. Work, Jonathan Sprinkle, Benedetto Piccoli, and Alexandre M. Bayen. Designing, simulating, and performing the 100-av field test for the circles consortium: Methodology and implementation of the largest mobile traffic control experiment to date. *preprint*, 2023.
- [3] Masako Bando, Katsuya Hasebe, Akihiro Nakayama, Akihiro Shibata, and Yuki Sugiyama. Dynamical model of traffic congestion and numerical simulation. *Physical review E*, 51(2):1035, 1995.
- [4] B. Baskar, B. De Schutter, and H. Hellendoorn. Model-based predictive traffic control for intelligent vehicles: Dynamic speed limits and dynamic lane allocation. *Proceedings of the 2008 IEEE Intelligent Vehicles Symposium (IV'08)*, pages 174–179, 2008.
- [5] Rahul Bhadani, Matt Bunting, Matthew Nice, Ngoc Minh Tran, Safwan Elmadani, Dan Work, and Jonathan Sprinkle. Strym: A python package for real-time can data logging, analysis and visualization to work with usb-can interface. In *2022 2nd Workshop on Data-Driven and Intelligent Cyber-Physical Systems for Smart Cities Workshop (DI-CPS)*, pages 14–23. IEEE, 2022.
- [6] Rahul Bhadani, Matthew Bunting, Matthew Nice, Fangyu Wu, Amaury Hayat, Jonathan Lee, Alexandre Bayen, Benedetto Piccoli, Benjamin Seibold, Dan Work, and Jonathan Sprinkle. Approaches for synthesis and deployment of controller models on automated vehicles for car-following in mixed autonomy. In *Proceedings of Cyber-Physical Systems and Internet of Things Week 2023*, pages 158–163. 2023.
- [7] Rahul Kumar Bhadani, Benedetto Piccoli, Benjamin Seibold, Jonathan Sprinkle, and Daniel Work. Dissipation of emergent traffic waves in stop-and-go traffic using a supervisory controller. In *2018 IEEE Conference on Decision and Control (CDC)*, pages 3628–3633. IEEE, 2018.
- [8] Rahul Kumar Bhadani, Jonathan Sprinkle, and Matthew Bunting. The CAT vehicle testbed: A simulator with hardware in the loop for autonomous vehicle applications. *Electronic Proceedings in Theoretical Computer Science*, 269:32–47, apr 2018.
- [9] Matt Bunting, Rahul Bhadani, Matt Nice, Safwan Elmadani, and Jonathan Sprinkle. Data from the development evolution of a vehicle for custom control. In *2022 2nd Workshop on Data-Driven and Intelligent Cyber-Physical Systems for Smart Cities Workshop (DI-CPS)*, pages 40–46. IEEE, 2022.

- [10] Matthew Bunting, Rahul Bhadani, and Jonathan Sprinkle. Libpanda: A high performance library for vehicle data collection. In *Proceedings of the Workshop on Data-Driven and Intelligent Cyber-Physical Systems*, pages 32–40, 2021.
- [11] L. C. Davis. Effect of adaptive cruise control systems on traffic flow. *Phys. Rev. E*, 69:066110, Jun 2004.
- [12] Maria Laura Delle Monache, Thibault Liard, Anaïs Rat, Raphael Stern, Rahul Bhadani, Benjamin Seibold, Jonathan Sprinkle, Daniel B Work, and Benedetto Piccoli. Feedback control algorithms for the dissipation of traffic waves with autonomous vehicles. *Computational Intelligence and Optimization Methods for Control Engineering*, pages 275–299, 2019.
- [13] Safwan Elmadani, Matthew Nice, Matthew Bunting, Jonathan Sprinkle, and Rahul Bhadani. From can to ros: A monitoring and data recording bridge. In *Proceedings of the Workshop on Data-Driven and Intelligent Cyber-Physical Systems*, pages 17–21, 2021.
- [14] Mauro Garavello, Paola Goatin, Thibault Liard, and Benedetto Piccoli. A multiscale model for traffic regulation via autonomous vehicles. *Journal of Differential Equations*, 269(7):6088–6124, 2020.
- [15] Denos C Gazis, Robert Herman, and Richard W Rothery. Nonlinear follow-the-leader models of traffic flow. *Operations research*, 9(4):545–567, 1961.
- [16] Vittorio Giammarino, Simone Baldi, Paolo Frasca, and Maria Laura Delle Monache. Traffic flow on a ring with a single autonomous vehicle: An interconnected stability perspective. *IEEE Transactions on Intelligent Transportation Systems*, 22(8):4998–5008, 2020.
- [17] Derek Gloudemans, William Barbour, Nikki Gloudemans, Matthew Neuendorf, Brad Freeze, Said El-Said, and Daniel B Work. Interstate-24 motion: Closing the loop on smart mobility. In *2020 IEEE Workshop on Design Automation for CPS and IoT (DESTION)*, pages 49–55. IEEE, 2020.
- [18] Derek Gloudemans, Yanbing Wang, Gracie Gumm, William Barbour, and Daniel B Work. The interstate-24 3d dataset: a new benchmark for 3d multi-camera vehicle tracking. *arXiv preprint arXiv:2308.14833*, 2023.
- [19] Derek Gloudemans, Yanbing Wang, Junyi Ji, Gergely Zachar, William Barbour, Eric Hall, Meredith Cebelak, Lee Smith, and Daniel B Work. I-24 motion: An instrument for freeway traffic science. *Transportation Research Part C: Emerging Technologies*, 155:104311, 2023.
- [20] Derek Gloudemans and Daniel B Work. Vehicle tracking with crop-based detection. In *2021 20th IEEE International Conference on Machine Learning and Applications (ICMLA)*, pages 312–319. IEEE, 2021.
- [21] Derek Gloudemans, Gergely Zachár, Yanbing Wang, Junyi Ji, Matt Nice, Matt Bunting, William Barbour, Jonathan Sprinkle, Benedetto Piccoli, Maria Laura Monache, Alexandre Bayen, Benjamin Seibold, and Daniel B. Work. So you think you can track? *arXiv preprint arXiv:2309.07268*, 2023.
- [22] Xiaoqian Gong and Alexander Keimer. On the well-posedness of the ”bando-follow the leader” car following model and a time-delayed version. *Networks and Heterogeneous Media*, 18(2):775–798, 2023.
- [23] Maxime Guériau, Romain Billot, Nour-Eddin [El Faouzi], Julien Monteil, Frédéric Armetta, and Salima Hassas. How to assess the benefits of connected vehicles? a simulation framework for the design of cooperative traffic management strategies. *Transportation Research Part C: Emerging Technologies*, 67:266 – 279, 2016.
- [24] Youngjun Han, Danjue Chen, and Soyoung Ahn. Variable speed limit control at fixed freeway bottlenecks using connected vehicles. *Transportation Research Part B: Methodological*, 98:113 – 134, 2017.
- [25] Amaury Hayat, Xiaoqian Gong, Jonathan Lee, Sydney Truong, Sean McQuade, Nicolas Kardous, Alexander Keimer, Yiling You, Saleh Albeaik, Eugene Vinistky, Paige Arnold, Maria Laura Delle Monache, Alexandre Bayen, Benjamin Seibold, Jonathan Sprinkle, Dan Work, and Benedetto Piccoli. *A Holistic Approach to the Energy-Efficient Smoothing of Traffic via Autonomous Vehicles*, pages 285–316. Springer International Publishing, Cham, 2022.

- [26] Amaury Hayat, Benedetto Piccoli, and Sydney Truong. Dissipation of traffic jams using a single autonomous vehicle on a ring road. *SIAM Journal on Applied Mathematics*, 83(3):909–937, 2023.
- [27] Amaury Hayat, Benedetto Piccoli, and Shengquan Xiang. An autonomous vehicle control to dissipate jams. *preprint*.
- [28] Z. He, L. Zheng, L. Song, and N. Zhu. A jam-absorption driving strategy for mitigating traffic oscillations. *IEEE Transactions on Intelligent Transportation Systems*, 18(4):802–813, 2017.
- [29] Nicolas Kardous, Amaury Hayat, Sean T. McQuade, Xiaoqian Gong, Sydney Truong, Tinhinane Mezair, Paige Arnold, Ryan Delorenzo, Alexandre Bayen, and Benedetto Piccoli. A rigorous multi-population multi-lane hybrid traffic model for dissipation of waves via autonomous vehicles. *The European Physical Journal Special Topics*, 231(9):1689–1700, 2022.
- [30] B. S. Kerner. *The physics of traffic: empirical freeway pattern features, engineering applications, and theory*. Springer, 2012.
- [31] Jonathan W. Lee, George Gunter, Rabie Ramadan, Sulaiman Almatrudi, Paige Arnold, John Aquino, William Barbour, Rahul Bhadani, Joy Carpio, Fang-Chieh Chou, Marsalis Gibson, Xiaoqian Gong, Amaury Hayat, Nour Khoudari, Abdul Rahman Kreidieh, Maya Kumar, Nathan Lichtlé, Sean McQuade, Brian Nguyen, Megan Ross, Sydney Truong, Eugene Vinitsky, Yibo Zhao, Jonathan Sprinkle, Benedetto Piccoli, Alexandre M. Bayen, Daniel B. Work, and Benjamin Seibold. Integrated framework of vehicle dynamics, instabilities, energy models, and sparse flow smoothing controllers. In *Proceedings of the Workshop on Data-Driven and Intelligent Cyber-Physical Systems*, DI-CPS’21, page 41–47, New York, NY, USA, 2021. Association for Computing Machinery.
- [32] Jonathan W. Lee, Han Wang, Kathy Jang, Amaury Hayat, Matthew Bunting, Arwa Alanqary, William Barbour, Zhe Fu, Xiaoqian Gong, George Gunter, Sharon Hornstein, Abdul Rahman Kreidieh, Nathan Lichtlé, Matthew W. Nice, William A. Richardson, Adit Shah, Eugene Vinistky, Fangyu Wu, Shengquan Xiang, Sulaiman Almatrudi, Fahd Althukair, Rahul Bhadani, Joy Carpio, Raphaël Chekroun, Eric Cheng, Maria Teresa Chiri, Fang-Chieh Chou, Ryan Delorenzo, Marsalis Gibson, Derek Gloudemans, Anish Gollakota, Junyi Ji, Alexander Keimer, Nour Khoudari, Malaika Mahmood, Mikail Mahmood, Hossein Nick Zinat Matin, Sean McQuade, Rabie Ramadan, Daniel Urieli, Xia Wang, Yanbing Wang, Rita Xu, Mengsha Yao, Yiling You, Gergely Zachár, Yibo Zhao, Mostafa Ameli, Mirza Najamuddin Baig, Sarah Bhaskaran, Kenneth Butts, Manasi Gowda, Caroline Janssen, John Lee, Liam Pedersen, Riley Wagner, Zimo Zhang, Chang Zhou, Daniel B. Work, Benjamin Seibold, Jonathan Sprinkle, Benedetto Piccoli, Maria Laura Delle Monache, and Alexandre M. Bayen. Traffic smoothing via connected & automated vehicles: A modular, hierarchical control design deployed in a 100-cav flow smoothing experiment. *preprint*, 2023.
- [33] Nathan Lichtlé, Eugene Vinitsky, Matthew Nice, Benjamin Seibold, Dan Work, and Alexandre M Bayen. Deploying traffic smoothing cruise controllers learned from trajectory data. In *2022 International Conference on Robotics and Automation (ICRA)*, pages 2884–2890. IEEE, 2022.
- [34] Matthew Nice, Matthew Bunting, Daniel Work, and Jonathan Sprinkle. Middleware for a heterogeneous cav fleet. In *Proceedings of Cyber-Physical Systems and Internet of Things Week 2023*, pages 86–91. 2023.
- [35] Ryosuke Nishi, Akiyasu Tomoeda, Kenichiro Shimura, and Katsuhiko Nishinari. Theory of jam-absorption driving. *Transportation Research Part B: Methodological*, 50:116 – 129, 2013.
- [36] Morgan Quigley, Ken Conley, Brian Gerkey, Josh Faust, Tully Foote, Jeremy Leibs, Rob Wheeler, Andrew Y Ng, et al. Ros: an open-source robot operating system. In *ICRA workshop on open source software*, volume 3, page 5. Kobe, Japan, 2009.
- [37] Raphael E. Stern, Yuche Chen, Miles Churchill, Fangyu Wu, Maria Laura Delle Monache, Benedetto Piccoli, Benjamin Seibold, Jonathan Sprinkle, and Daniel B. Work. Quantifying air quality benefits

- resulting from few autonomous vehicles stabilizing traffic. *Transportation Research Part D: Transport and Environment*, 67:351–365, 2019.
- [38] Raphael E. Stern, Shumo Cui, Maria Laura Delle Monache, Rahul Bhadani, Matt Bunting, Miles Churchill, Nathaniel Hamilton, R’mani Haulcy, Hannah Pohlmann, Fangyu Wu, Benedetto Piccoli, Benjamin Seibold, Jonathan Sprinkle, and Daniel B. Work. Dissipation of stop-and-go waves via control of autonomous vehicles: Field experiments. *Transportation Research Part C: Emerging Technologies*, 89:205–221, 2018.
- [39] Yuki Sugiyama, Minoru Fukui, Macoto Kikuchi, Katsuya Hasebe, Akihiro Nakayama, Katsuhiko Nishinari, Shin-ichi Tadaki, and Satoshi Yukawa. Traffic jams without bottlenecks—experimental evidence for the physical mechanism of the formation of a jam. *New journal of physics*, 10(3):033001, 2008.
- [40] Alireza Talebpour and Hani S. Mahmassani. Influence of connected and autonomous vehicles on traffic flow stability and throughput. *Transportation Research Part C: Emerging Technologies*, 71:143 – 163, 2016.
- [41] J. TREITERER and J. MYERS. The hysteresis phenomenon in traffic flow. In *Proceedings of the 6th International Symposium on Transportation and Traffic Theory, Sydney, Australia*, 1974.
- [42] Eugene Vinitsky, Aboudy Kreidieh, Luc Le Flem, Nishant Kheterpal, Kathy Jang, Cathy Wu, Fangyu Wu, Richard Liaw, Eric Liang, and Alexandre M Bayen. Benchmarks for reinforcement learning in mixed-autonomy traffic. In *Conference on robot learning*, pages 399–409. PMLR, 2018.
- [43] M. Wang, W. Daamen, S. P. Hoogendoorn, and B. van Arem. Cooperative car-following control: Distributed algorithm and impact on moving jam features. *IEEE Transactions on Intelligent Transportation Systems*, 17(5):1459–1471, 2016.
- [44] Meng Wang, Winnie Daamen, Serge P. Hoogendoorn, and Bart van Arem. Connected variable speed limits control and car-following control with vehicle-infrastructure communication to resolve stop-and-go waves. *Journal of Intelligent Transportation Systems*, 20(6):559–572, 2016.
- [45] Yanbing Wang, Derek Gloudemans, Zi Nean Teoh, Lisa Liu, Gergely Zachár, William Barbour, and Daniel Work. Automatic vehicle trajectory data reconstruction at scale. *arXiv preprint arXiv:2212.07907*, 2022.
- [46] Yanbing Wang, Junyi Ji, William Barbour, and Daniel B Work. Online min cost circulation for multi-object-tracking on fragments. In *2023 IEEE International Intelligent Transportation Systems Conference (ITSC)*. IEEE, 2023. To appear.
- [47] Cathy Wu, Abdul Rahman Kreidieh, Kanaad Parvate, Eugene Vinitsky, and Alexandre M Bayen. Flow: A modular learning framework for mixed autonomy traffic. *IEEE Transactions on Robotics*, 38(2):1270–1286, Jul 2021.
- [48] Cathy Wu, Aboudy Kreidieh, Kanaad Parvate, Eugene Vinitsky, and Alexandre M Bayen. Flow: Architecture and benchmarking for reinforcement learning in traffic control. *arXiv preprint arXiv:1710.05465*, 10, 2017.
- [49] Cathy Wu, Aboudy Kreidieh, Eugene Vinitsky, and Alexandre M. Bayen. Emergent behaviors in mixed-autonomy traffic. In *Conference on Robot Learning (CoRL)*, 2017.
- [50] Fangyu Wu, Raphael E. Stern, Shumo Cui, Maria Laura [Delle Monache], Rahul Bhadani, Matt Bunting, Miles Churchill, Nathaniel Hamilton, R’mani Haulcy, Benedetto Piccoli, Benjamin Seibold, Jonathan Sprinkle, and Daniel B. Work. Tracking vehicle trajectories and fuel rates in phantom traffic jams: Methodology and data. *Transportation Research Part C: Emerging Technologies*, 99:82 – 109, 2019.
- [51] Zhongxia Yan, Abdul Rahman Kreidieh, Eugene Vinitsky, Alexandre M. Bayen, and Cathy Wu. Unified automatic control of vehicular systems with reinforcement learning. *IEEE Transactions on Automation Science and Engineering*, page 1–16, Apr 2022.

- [52] Gergely Zachár. Visualization of large-scale trajectory datasets. CPS-IoT Week '23, page 152–157, New York, NY, USA, 2023. Association for Computing Machinery.